Novel Vector Design and Hexosaminidase Variant Enabling Self-Complementary Adeno-Associated Virus for the Treatment of Tay-Sachs Disease

Subha Karumuthil-Melethil,[1] Sahana Nagabhushan Kalburgi,[1] Patrick Thompson,[2] Michael Tropak,[3] Michael D. Kaytor,[4] John G. Keimel,[4] Brian L. Mark,[5] Don Mahuran,[3,6] Jagdeep S. Walia,[2] and Steven J. Gray[1,7,*]

[1]Gene Therapy Center, University of North Carolina at Chapel Hill, Chapel Hill, North Carolina; [2]Medical Genetics/Departments of Pediatrics, Queen's University, Kingston, Ontario, Canada; [3]Genetics and Genome Biology, SickKids, Toronto, Ontario, Canada; [4]New Hope Research Foundation, North Oaks, Minnesota; [5]Department of Microbiology, University of Manitoba, Winnipeg, Manitoba, Canada; [6]Department of Laboratory Medicine and Pathology, University of Toronto, Toronto, Ontario, Canada; and [7]Department of Ophthalmology, University of North Carolina at Chapel Hill, Chapel Hill, North Carolina.

G_{M2} gangliosidosis is a family of three genetic neurodegenerative disorders caused by the accumulation of G_{M2} ganglioside (G_{M2}) in neuronal tissue. Two of these are due to the deficiency of the heterodimeric (α–β), "A" isoenzyme of lysosomal β-hexosaminidase (HexA). Mutations in the α-subunit (encoded by *HEXA*) lead to Tay-Sachs disease (TSD), whereas mutations in the β-subunit (encoded by *HEXB*) lead to Sandhoff disease (SD). The third form results from a deficiency of the G_{M2} activator protein ($G_{M2}AP$), a substrate-specific cofactor for HexA. In their infantile, acute forms, these diseases rapidly progress with mental and psychomotor deterioration resulting in death by approximately 4 years of age. After gene transfer that overexpresses one of the deficient subunits, the amount of HexA heterodimer formed would empirically be limited by the availability of the other endogenous Hex subunit. The present study used a new variant of the human HexA α-subunit, μ, incorporating critical sequences from the β-subunit that produce a stable homodimer (HexM) and promote functional interactions with the $G_{M2}AP$– G_{M2} complex. We report the design of a compact adeno-associated viral (AAV) genome using a synthetic promoter–intron combination to allow self-complementary (sc) packaging of the *HEXM* gene. Also, a previously published capsid mutant, AAV9.47, was used to deliver the gene to brain and spinal cord while having restricted biodistribution to the liver. The novel capsid and cassette design combination was characterized *in vivo* in TSD mice for its ability to efficiently transduce cells in the central nervous system when delivered intravenously in both adult and neonatal mice. This study demonstrates that the modified HexM is capable of degrading long-standing G_{M2} storage in mice, and it further demonstrates the potential of this novel scAAV vector design to facilitate widespread distribution of the *HEXM* gene or potentially other similar-sized genes to the nervous system.

INTRODUCTION

TAY-SACHS DISEASE (TSD) is one of a group of three lysosomal storage diseases called G_{M2} gangliosidosis, caused by defective catabolism of G_{M2} ganglioside (G_{M2}). It is an autosomal recessive neurodegenerative disease caused by mutations in the α-subunit of the heterodimeric enzyme β-hexosaminidase A (HexA). Sandhoff disease (SD) is caused by mutations in the β-subunit of HexA. Both subunits can also form functional homodimers, HexS (α–α) and HexB (β–β), which in

humans cannot significantly turn over G_{M2}. HexS is unstable and physiologically less significant, whereas HexB is highly stable and can degrade some neutral glycolipids, oligosaccharides, and artificial substrates. The enzyme HexA (α–β) requires a substrate-specific cofactor, called G_{M2} activator protein ($G_{M2}AP$), to efficiently degrade G_{M2}. Mutations to the gene encoding $G_{M2}AP$ lead to another rare variant of G_{M2} gangliosidosis, the AB-variant form. The characteristic histopathological feature of these diseases is the presence of swollen neurons

and neuronal distortion throughout the nervous system caused by accumulated G_{M2}. TSD and SD are clinically variable, with severe forms showing profound mental retardation and death within 2–3 years of birth.[1] Heterogeneity of the disease regarding severity of clinical signs and age of onset can be attributed to the level of residual HexA activity allowed by different mutations. It has been estimated that only between 10 and 15% of normal HexA activity is needed to prevent G_{M2} accumulation.[2] At present, there are no effective treatment options available for these diseases.

To study the disease mechanisms and to test various therapeutic approaches, mouse models have been developed for both these diseases. The mouse model for TSD, developed by the targeted disruption of the *hexa* gene encoding the α-subunit,[3–5] has no or a mild behavioral phenotype but displays many of the neuropathological features characteristic of TSD, in particular G_{M2} ganglioside accumulation. The absence of clinical signs in TSD mice is due to the presence of a lysosomal mouse sialidase capable of hydrolyzing G_{M2} to its neutral asialo derivative, G_{A2}, which then interacts with HexB to be further degraded to glucosylceramide.[5,6] This alternative metabolic pathway helps TSD mice to keep G_{M2} accumulation below an acutely toxic level and thereby escape clinical symptoms. The $hexb^{-/-}$ mouse model for Sandhoff disease exhibits a severe disease phenotype as it is deficient in both HexA and HexB and has extensive G_{M2} accumulation throughout the brain and spinal cord with a humane end point of approximately 16 weeks of age.[4,5]

Several gene replacement therapies have been tested in the mouse models for these diseases. The heterodimeric nature of HexA, which is the only isoenzyme capable of degrading G_{M2}, makes the treatment for TSD and SD more challenging. Adenoviral gene therapy of TSD mice, using a vector encoding *HEXA* alone, when injected intravenously produced only a slight increase in HexA (or possibly HexS mistaken for HexA) activity in the serum, whereas simultaneous injection of vectors encoding both *HEXA* and *HEXB* increased the serum HexA activity to 42% of wild-type levels in these mice.[7] SD mice injected intracranially with a recombinant adeno-associated viral (rAAV) vector expressing the β-subunit, or a combination of vectors with α- and β-subunits, showed reduction in G_{M2} levels and increased survival.[8] However, the effect of the single-subunit vector in this study could be attributed to higher levels of HexB and the mouse sialidase driving the alternative metabolic pathway for hydrolyzing G_{M2}. A single striatal injection of a mixture of vectors expressing the β-hexosaminidase

α- and β-subunits in SD mice prevented the neuronal loss in the brain.[9] Cachon-Gonzalez and colleagues reported that intracranial coinjection of rAAV vectors expressing the α- and β-subunits into 1-month-old SD mice prevented the disease pathology throughout the brain and spinal cord, which helped the mice survive up to 2 years.[10] In that study, an infusion of an rAAV vector encoding the β-subunit alone resulted in detectable expression of only the HexB isozyme. AAVrh8 vectors encoding feline α- and β-subunits were injected intracranially into SD cats at a 1:1 ratio, and this resulted in a significant reduction in cerebrospinal fluid (CSF) biomarkers of the disease. It ultimately resulted in extension of the life span for the treated cats.[11] Intracranial stereotaxic infusion of a mixture of rAAV2/1α and rAAV2/1β into 4-week-old SD mice extended the median survival from 131 to 615 days.[12]

The gene replacement therapies so far discussed all used direct injections to the brain, using viral vectors. The possibility of translating this highly invasive delivery approach into humans is problematic simply given the size differential between the brains of animal models and humans, along with the limited spread of AAV vectors from the injection site. The emergence of AAV9 vectors for global gene transfer into the brain and spinal cord, due to its ability to penetrate the blood–brain barrier, has resulted in therapeutic approaches for multiple CNS diseases via intravascular gene delivery.[13–17] Intravenous administration of self-complementary AAV9 vectors has been demonstrated as a viable and translatable approach to target the CNS in mice, cats, and non-human primates,[18–21] and this approach is being applied in a human trial for spinal muscular atrophy (clinicaltrials.gov identifier NCT02122952). These studies demonstrating the ability of AAV9 to achieve widespread CNS transduction all relied on the more efficient, self-complementary AAV (scAAV), vector design. scAAV vectors have been shown to be greater than 10-fold more efficient in transducing cells, compared with traditional single-stranded AAV (ssAAV) vectors when tested *in vivo*.[18,22] The drawback of using an scAAV vector is the restricted packaging capacity of approximately 2.2 kb of foreign DNA, making it difficult to package larger genes along with regulatory expression elements. In a review by Powell and colleagues,[23] they listed the relative strength and size of various promoters and polyadenylation [poly(A)] signals. Among the widely used ubiquitous promoters, the cytomegalovirus (CMV) early enhancer/chicken β-actin (CBA or CAGGS) promoter (1600 bp), the related hybrid chicken β-actin (CBh) promoter (800 bp), and the CMV enhancer/promoter (800 bp) are all too large to accommodate a

HEX gene in an scAAV vector. Small enhancerless promoters such as UbC, MeCP2, and GUSB could accommodate the size of the *HEX* gene, but would likely provide inadequate levels of expression. At present, no publication has described an scAAV vector design capable of packaging the approximately 1.6-kb *HEXA* or *HEXB* gene to treat TSD or SD.

An ideal vector capable of treating TSD and SD would express both *HEXA* and *HEXB* genes simultaneously, but this would be beyond the packaging capacity of scAAV, which is needed to achieve efficient global CNS gene transfer. Therefore, there is a conceptual advantage to creating an engineered subunit that could be delivered, using a single scAAV vector, and that could form a stable and functional homodimer when delivered *in vivo* and degrade G_{M2} in a G_{M2}AP-dependent manner. The crystallographic structures of human HexA and HexB have been elucidated in detail.[24,25] Matsuoka and colleagues attempted to design and develop a modified HexB reported to have G_{M2}-degrading activity and G_{M2}AP-binding ability, based on the amino acid homology between the Hex α- and β-subunits.[26] They purified the modified HexB recombinant enzyme with the altered substrate specificity, that is, the ability to efficiently bind negatively charged substrates, and an α-loop sequence for enhancing its interaction with the G_{M2}AP–G_{M2} complex. They administered the modified HexB by intracerebroventricular injection directly to the CNS of 10-week-old SD mice and observed a remarkable reduction in G_{M2} storage in the thalamus, cerebral cortex, and also the liver. Their results indicated that the modified HexB enzyme can function *in vivo* if used in enzyme replacement therapy (ERT). However, Sinici and colleagues[27] tested this construct and another more extensive hybrid β-subunit construct *in cellulo*, using Tay-Sachs cells preloaded with a fluorescent G_{M2} derivative, and found that neither modified β-subunit was capable of significant human G_{M2}AP-dependent hydrolysis of G_{M2}. Likely, the encouraging results reported by Matsuoka and colleagues are attributable to restoration of HexB-like activity that takes advantage of the alternative sialidase pathway in mice. As an alternative approach to develop a hybrid subunit, Tropak and colleagues[28] designed a modified α-subunit incorporating both the unique β-subunit sequences required to form a stable, HexB-like, homodimer and those sequences needed for the homodimer to interact with the G_{M2}AP–G_{M2} complex. The α-active site was retained in order to facilitate the hydrolysis of negatively charged substrates, for example, G_{M2}. This modified subunit (μ) was confirmed to form a stable dimeric enzyme,

HexM, which could bind to the G_{M2}AP–G_{M2} complex, and degrade G_{M2} in live human embryonic kidney (HEK) cells rendered HEXA$^{-/-}$ and HEXB$^{-/-}$ by CRISPR (clustered regularly interspaced short palindromic repeats) gene editing. *In vivo* experiments in this study further demonstrated the ability of HexM to reduce accumulated G_{M2} in Tay-Sachs and Sandhoff mice. Therefore, this homodimer has HexA-like activity and can be expressed from a single gene packageable within an scAAV vector. This construct is discussed further in the present study.

It is important to note that systemic delivery of AAV9 vectors results in substantially higher biodistribution to the liver compared with the CNS, which could lead to transgene-specific liver toxicity.[15,29] Furthermore, some studies have reported incidence of liver tumors with intravenous delivery of AAV9 into neonates.[14,30,31] A liver-detargeted version of AAV9 with comparable levels of brain and spinal cord transduction could be a safer reagent to treat neurological disorders. Pulicherla and colleagues[32] reported the generation of AAV9-derived vectors displaying selective loss of liver tropism. One AAV9 variant, denoted as AAV9.47 with four point mutations (S414N, G453D, K557E, and T582I), showed a significant 110-fold decrease in the liver transduction in mice injected via the tail vein and analyzed 4 weeks postinjection by vector DNA biodistribution and transgene (luciferase) expression. The transduction pattern in the brain did not show any significant drop, which suggests AAV9.47 as a good candidate for global gene delivery to the CNS via systemic injection.

In the present study, we discuss the functional ability of the new hexosaminidase variant HexM and the design of a novel expression cassette to package it into an scAAV vector for *in vivo* applications. We show that the novel cassette has the ability to provide ubiquitous transduction throughout the CNS. We provide further characterization of the liver-detargeted AAV9.47 variant to demonstrate its ability to transduce neurons and glia throughout the CNS after intravenous injection into neonatal and adult mice. We demonstrate that the HexM homodimer is capable of degrading G_{M2} in a localized manner when injected intracranially into adult TSD mice, and that the scAAV9.47/*HEXM* vector can mediate long-term G_{M2} reduction when injected intravenously into neonatal TSD mice.

MATERIALS AND METHODS
Plasmid constructs

The plasmids carrying the transgene cassette required for packaging into scAAV vectors were designed for *GFP*, *HEXA*, and *HEXM*. This novel

design includes the combination of a short synthetic and ubiquitous promoter derived from the JeT promoter[33] and a synthetic intron (UsP, also referred to as the JeTI promoter) along with the simian virus 40 polyadenylation signal [SV40 poly(A)] to drive expression of the encoded gene (Fig. 1). A Kozak consensus sequence was incorporated at the start codon. Pilot *in vitro* studies showed that the UsP expression cassette had approximately 15% of the activity when using a CMV promoter (Supplementary Fig. S1; supplementary methods and data are available online at www.liebertpub.com/hum). The nucleotide sequence of the synthetic JeT promoter and intron is provided in Supplementary Fig. S2.

The human *HEXA* and *HEXM* genes were codon-optimized by DNA2.0 (Menlo Park, CA). The construct expressing GFP from the CBh promoter[22] with the bovine growth hormone (BGH) poly(A) was used as a reference standard for comparative gene expression for the newly designed constructs.

Vector preparation

Recombinant AAV vectors were generated as described,[34] using proprietary methods developed at the University of North Carolina Gene Therapy Center Vector Core facility (Chapel Hill, NC). The following AAV9 or AAV9.47 vectors were produced and used for this study: AAV9/CBh-*GFP*, AAV9.47/CBh-*GFP*, AAV9/UsP-*GFP*, AAV9/UsP-*HEXA*, AAV9/UsP-*HEXM*, AAV9.47/UsP-*GFP*, and AAV9.47/UsP-*HEXM*. All of these were scAAV vectors. Peak fractions were dialyzed in phosphate-buffered saline (PBS) containing 5% D-sorbitol and 350 mM NaCl. Viral titers were determined by qPCR as described.[35]

Mouse studies

All investigations were approved by the University of North Carolina–Chapel Hill Institutional Animal Care and Use Committee. The Tay-Sachs disease mouse model [strain B6;129S-*hexa*$^{-/-}$][3] and wild-type C57BL/6 mice were purchased from the Jackson Laboratory (Bar Harbor, ME) and bred at the University of North Carolina.

For intravenous delivery into wild-type adult female C57BL/6 mice, 200 μl of scAAV9/*GFP* (2×10^{11} VG) or AAV9.47/*GFP* (2×10^{11} VG) was injected and expression/biodistribution was analyzed 3–4 weeks postinjection. Adult TSD knockout mice were injected via the tail vein with scAAV9.47/*GFP* (5×10^{11} VG) in a volume of 200 μl when 4–5 months old and were analyzed 6 months postinjection.

Neonatal facial vein injections into TSD mice were performed on postnatal days 0–2 (P0–P2), using scAAV9.47/UsP-*GFP* (5×10^{10} VG) or scAAV9.47/UsP-*HEXM* (5×10^{10} VG) in a volume of 20 μl. The injections were carried out before the genotypes of the mice were determined and as such included both heterozygous and knockout mice. They were euthanized when 15 months old.

Intracranial injections were performed as described[35] into 15-month-old TSD knockout mice, using the following stereotaxic coordinates, relative to bregma: rostral/caudal, +0.5 mm (toward rostral); left/right: left, +3 mm; up/down, −4 mm. These mice received a mixture of AAV9/*GFP* (1×10^9 VG) and either AAV9/*HEXM* (1×10^9 VG) or AAV9/*HEXA* (1×10^9 VG) in a total volume of 1 μl delivered over 10 min. Two mice were injected per vector mixture. They were analyzed 4 weeks postinjection. At sacrifice, the mice were transcardially perfused with PBS containing heparin at 1 U/ml (Abraxis, Schaumburg, IL) and samples were collected for downstream analysis.

Immunohistochemistry

After 48 hr of fixation in freshly made PBS containing 4% paraformaldehyde, the entire brain and portions of the cervical and lumbar spinal cords were sectioned at 40 μm, using a Leica vibrating microtome. Every fifth section was processed for immunohistochemistry (IHC). Sections were treated with hydrogen peroxide to remove endogenous peroxidase activity before blocking. Samples were incubated for 1 hr at room temperature in blocking solution (10% goat serum, 0.1% Triton X-100, 1×PBS) and then incubated for 48–72 hr at 4°C in primary antibody solution (3% goat serum, 0.1% Triton X-100, 1×PBS, and primary antibody). Primary antibodies were as follows: rabbit anti-GFP (diluted 1:1000; #AB3080, Millipore, Bedford, MA) or the human anti-G$_{M2}$ ganglioside antibody (diluted 1:1000; KM966, gift from Kyowa Hakko Kirin, Tokyo, Japan). After incubating with the appropriate
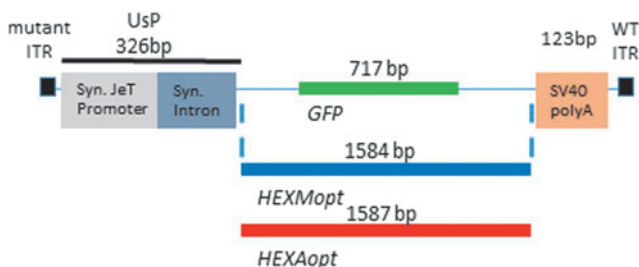

Figure 1. Adeno-associated viral (AAV) construct diagrams. The expression cassette design for packaging *GFP* and codon-optimized versions of human *HEXA* and *HEXM* included a novel synthetic promoter–intron combination (UsP) along with the simian virus 40 polyadenylation signal (SV40 polyA) to drive expression. These elements are flanked by the mutant inverted terminal repeat (ITR) on the 5′ end and the wild-type (WT) AAV2 ITR on the 3′ end to package into a self-complementary AAV vector. Color images available online at www.liebertpub.com/hum

secondary antibody for 1 hr at room temperature, color development was performed with a VECTAS-TAIN Elite ABC kit (#PK-6100; Vector Laboratories, Burlingame, CA) with 3,3′-diaminobenzidine tetrachloride (DAB) (#04008; Polysciences, Warrington, PA) substrate and nickel–cobalt intensification of the reaction product.

DAB-processed brain sections were digitized with a ScanScope slide scanner (Aperio Technologies, Vista, CA). Virtual slides were viewed with the ImageScope software package (version 10.0; Aperio Technologies).

For the data provided in Supplementary Fig. S3B, a region of interest was created in three representative images of an identical cortex area of the brain per vector treatment, and the number of astrocytes and neurons (identified by morphology) were manually counted. The results from two independent counters were averaged. Data are expressed as number of cells per millimeter squared.

Quantitative PCR analysis of vector genomes

Quantitative PCR (qPCR) was used for vector biodistribution studies. Tissue DNA was purified and quantified as described.[18] Data are reported as the number of double-stranded *GFP* or *HEXM* DNA molecules per two double-stranded copies of the murine *LaminB2* locus, or in other words, the number of vector DNA copies per diploid mouse genome.

Biochemical detection of G_{M2} gangliosides

Gangliosides were extracted by a modification of a method described earlier.[36] Briefly, previously frozen murine mid-brain sections were weighed and sonicated in 0.5 ml of methanol at amplitude 15–20% for 3×10 sec pulses with cooling on ice between pulses (Sonic Dismembrator model 500; Fisher Scientific, Waltham, MA). Samples were centrifuged for 15 min at 10,000 rpm at 4°C, and 0.4 ml of supernatant was removed for enzyme activity studies; the remainder was suspended (including the pellet) up to a final volume of 1.5 ml of methanol added to 2.5 ml of chloroform. Acidic gangliosides were isolated using C_{18}-E columns (Phenomenex, Torrance, CA) and eluted sequentially in 2 ml of methanol, and then in 2 ml of a 1:1 methanol–chloroform mixture. The eluate was then evaporated under a stream of nitrogen, and the residue was resuspended in 1:1 methanol–chloroform and then applied to an HPTLC silica gel 60 plate (Merck, Darmstadt, Germany) by applying $10\,\mu l$ at a time and drying between applications. Plates were developed with running buffer (chloroform–methanol–$CaCl_2$, 0.22% [55:45:10]). After staining with orcinol (Sigma-Aldrich, St. Louis, MO) and baking at 105°C

for 10 min, plates were immediately scanned for subsequent spot densitometric analysis (ImageJ software), with a mix of monosialoganglioside standards (Matreya, Pleasant Gap, PA) alongside. The ganglioside ratios are presented as G_{M2}:total gangliosides.

RESULTS

Liver-detargeted AAV9.47 capsid transduces neural cells after intravenous administration in adult mice

AAV9.47 capsid was engineered as described.[32] It was categorized as a liver-detargeted version of the AAV9 capsid, with a significant 110-fold decrease in liver transduction relative to the naturally occurring AAV9 capsid. The level of overall brain transduction was comparable to that of the original AAV9 capsid, making it a good candidate for targeted delivery to brain and other CNS organs via the intravenous route while avoiding the high biodistribution of AAV9 to the liver. The liver-detargeted characteristics of the AAV9.47 vector reported previously were confirmed in our study by a biodistribution study (Supplementary Fig. S3A). However, previous studies did not identify which cell types were transduced by AAV9.47 within the CNS. In our study, we observed that the capsid is able to transduce neural cells, predominantly neurons, when delivered intravenously into adult wild-type mice (Fig. 2B and Supplementary Fig. S4). GFP expression was visible throughout various regions of the brain and spinal cord. When compared with the transduction profile of AAV9 capsid packaged with the same transgene cassette containing GFP under the control of the CBh promoter and injected into wild-type mice (Fig. 2A), there was an approximately 4-fold reduction in the number of astrocytes transduced by the AAV9.47 capsid and an approximately 50% increase in the number of transduced neurons in the cortex (Supplementary Fig. S3B). Overall, AAV9.47 transduced approximately 20% less cells than AAV9 in the cortex.

Synthetic UsP promoter–intron drives ubiquitous expression in the brain

Previously, our laboratory described the use of a modified β-actin promoter with a shortened MVM (minute virus of mice) intron to drive sustained high levels of transgene expression in both neurons and glia throughout the CNS.[22] Combined with the BGH poly(A) signal, this scAAV construct can package a transgene of up to approximately 1.2 kb in length. The *HEXA* and *HEXM* transgenes are approximately 1.6 kb in length, requiring a novel expression cassette to
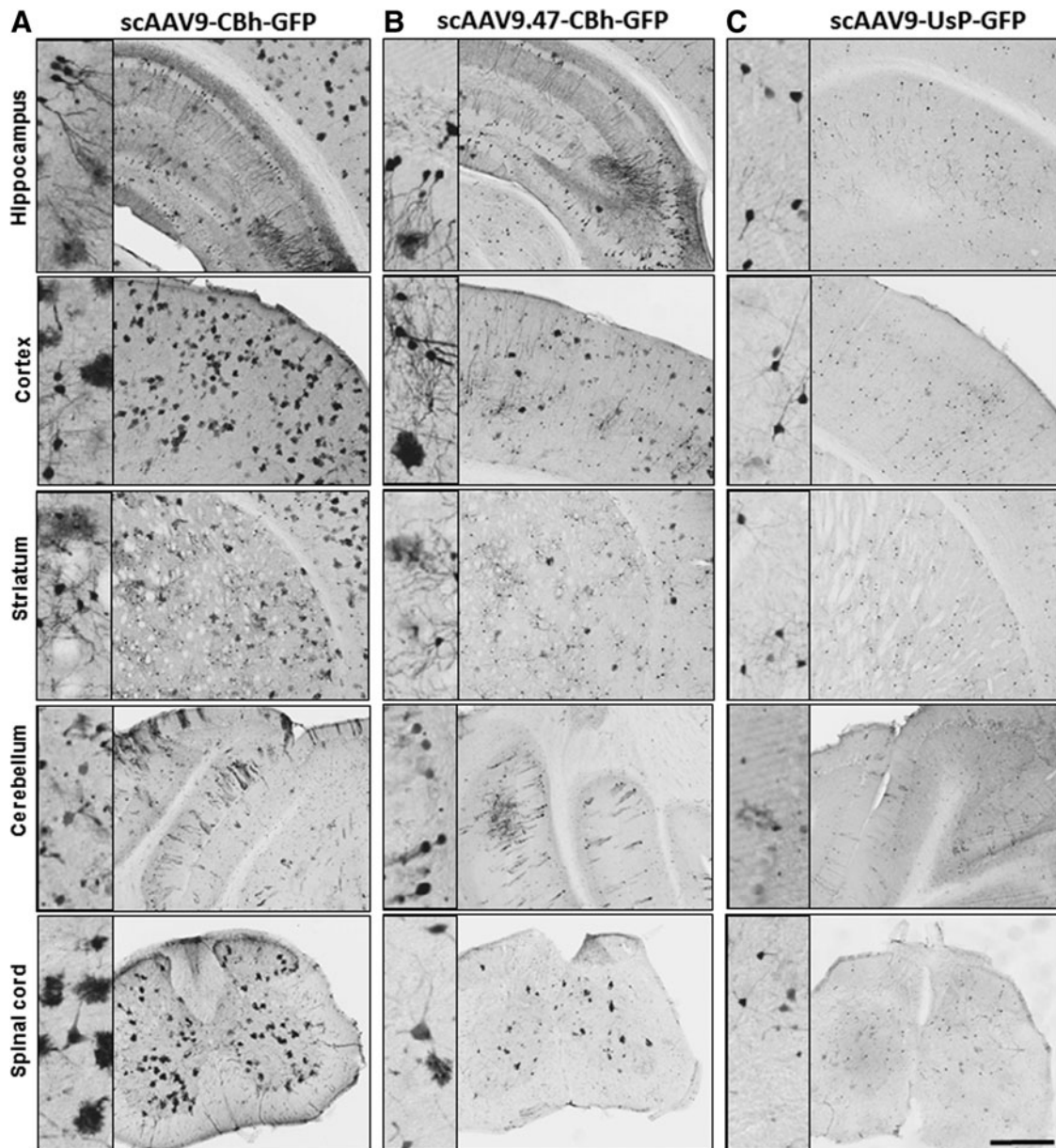
Figure 2. CNS transduction pattern of AAV9/CBh-*GFP*, AAV9.47/CBh-*GFP*, and AAV9/UsP-*GFP* after intravenous administration in wild-type mice. Adult wild-type mice were injected intravenously with 2×10^{11} vector genomes (VG) of scAAV9/CBh-*GFP* **(A)**, scAAV9.47/CBh-*GFP* **(B)**, or scAAV9/UsP-*GFP* **(C)** and then were euthanized 3 weeks postinjection to assess green fluorescent protein (GFP) transduction levels in various parts of the brain and spinal cord. Scale bar: 500 μm. *Insets:* An additional $\times 5$ magnification. All images are representative of at least three mice.

provide efficient and ubiquitous expression within the contexts of an scAAV genome. The newly designed expression cassette (Fig. 1), using the synthetic UsP promoter–intron combination, paired with the SV40 poly(A) signal, is capable of widespread expression in the CNS (Fig. 2C and Supplementary Fig. S4) after intravenous delivery in wild-type mice. The intensity of GFP expression in astrocytes is noticeably decreased for the UsP-GFP construct, compared with the CBh-GFP construct, when both were packaged in the AAV9 capsid. However, the novel design has the advantage of

being capable of packaging a transgene up to approximately 1.7 kb within an scAAV vector, which will accommodate the *HEXA* or *HEXM* transgene.

AAV9.47 capsid is capable of widespread gene transfer to the brain after intravenous administration in both adult and neonatal Tay-Sachs mice

To assess the ability of the UsP construct to mediate long-term sustained expression in the Tay-Sachs mouse model, we packaged the newly designed UsP-GFP construct within the AAV9.47

capsid and injected it intravenously into adult TSD mice at 4–5 months of age and into neonatal mice, consisting of both TSD and their heterozygous littermates, at age P0–P2. These mice were euthanized 6 and 15 months postinjection, respectively, and were analyzed for the biodistribution of the AAV vector by qPCR and for CNS transduction by IHC against GFP. As previously reported, the vector was significantly detargeted from the liver compared with the biodistribution pattern of AAV9,[18,32] while retaining biodistribution to the brain and spinal cord (Figs. 3A and 4A). IHC images of the brain clearly showed that the AAV9.47 capsid can deliver the gene to all regions of brain and facilitate expression in neurons and

glia within the CNS of $hexa^{-/-}$ and $hexa^{+/-}$ mice, and that this expression persisted for 15 months (Figs. 3B and 4B).

The hexosaminidase variant, HexM, can clear G_{M2} storage similar to HexA after intracranial administration into aged Tay-Sachs mice

To directly test the expression of the new hexosaminidase gene variant, *HEXM*, to reduce longstanding accumulated G_{M2} in the TSD mouse brain, compared with that of the unmodified *HEXA* gene, these were packaged into scAAV9 vectors and injected stereotaxically into 15-month-old TSD mice along with an identical titer of scAAV9/UsP-*GFP* vector to track vector spread. Each experimental
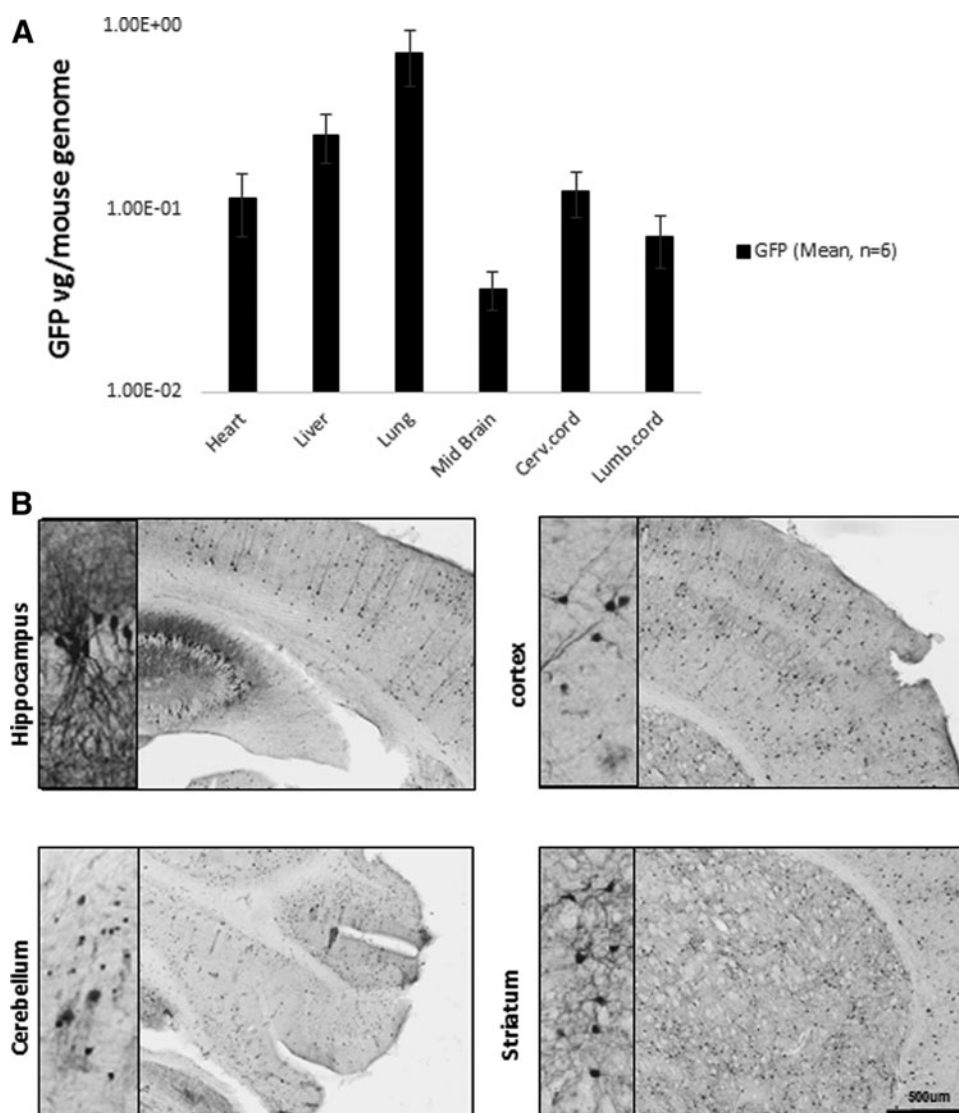

Figure 3. Biodistribution and brain transduction after intravenous administration of AAV9.47/UsP-*GFP* in adult Tay-Sachs mice. Adult Tay-Sachs knockout mice were injected intravenously when 4–5 months old with 5×10^{11} VG of scAAV9.47/UsP-*GFP* and analyzed 6 months postinjection. **(A)** The average number of GFP vector genomes in major organs from six mice. Error bars indicate the SEM. **(B)** Immunohistochemical (IHC) images from various regions of the brain from TSD mice showing GFP expression. Scale bar: 500 μm. *Insets:* An additional $\times 5$ magnification. The images are representative of four mice.
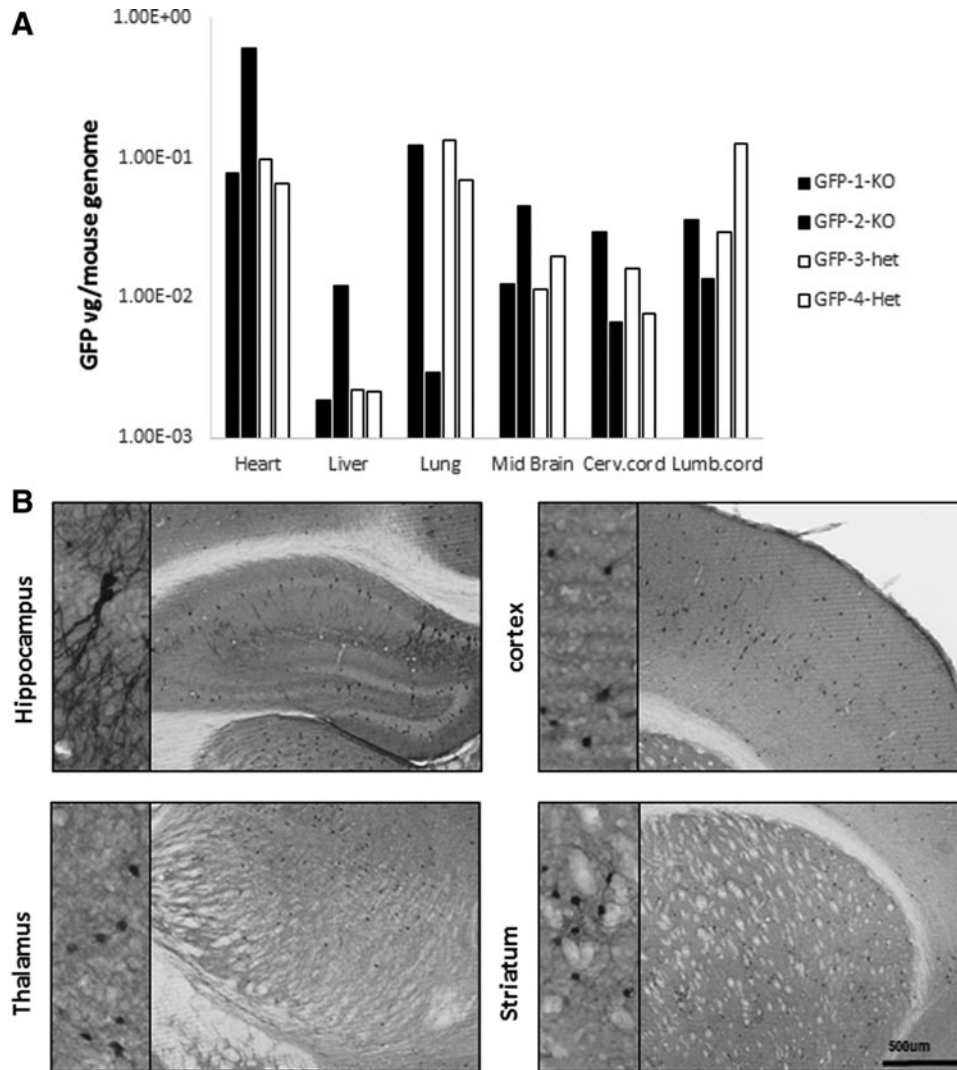
Figure 4. Vector biodistribution and immunohistochemical analysis after intravenous administration of scAAV9.47/UsP-*GFP* in neonatal Tay-Sachs mice. Tay-Sachs mice, both knockout (KO) and heterozygous (het), were injected via the facial vein on postnatal days 0–2 (P0–P2) with 5×10^{10} VG of scAAV9.47/UsP-*GFP* and analyzed 15 months postinjection. **(A)** qPCR biodistribution of GFP vector genomes in major organs in two heterozygous and two KO mice. **(B)** IHC images from various regions of the brain from a Tay-Sachs disease (TSD) KO mouse showing GFP expression. Scale bar: 500 μm. *Insets:* An additional $\times$5 magnification.

group consisted of two animals receiving the same vector combination. The mice were euthanized 4 weeks postinjection and the brain sections were subjected to IHC analysis against GFP and G_{M2} simultaneously. Several paired images of similar brain regions were analyzed. The HexA-like activity was assessed by the clearance of G_{M2} within the injected region, compared with the contralateral brain hemisphere (Fig. 5E–G). The area of AAV transduction was visualized by staining for GFP (Fig. 5A–C). Qualitatively, a marked reduction of G_{M2} was apparent in the areas that overlapped with strong GFP expression. Both β-hexosaminidase vectors were able to degrade G_{M2} in the regions that were injected, but complete clearance of accumulated G_{M2} was not obtained by either vector. IHC analysis was done on

brain sections from age-matched untreated heterozygous mice (Fig. 5D and H) for comparison with the G_{M2} levels in an unaffected brain. From these experiments, we conclude that delivery of scAAV9/UsP-*HEXM* results in clearance of long-standing G_{M2} accumulations, at least as well as that after delivery of scAAV9/UsP-*HEXA*.

Intravenous administration of AAV9.47/HEXM vector into neonatal Tay-Sachs mice results in long-term CNS reduction in G_{M2} gangliosides

Injections of AAV9.47/UsP-*HEXM* (at a dose of 5×10^{10} VG, through the facial vein) into neonatal TSD mice on P0–P2 were done; the mice included both knockout and heterozygous mice and were
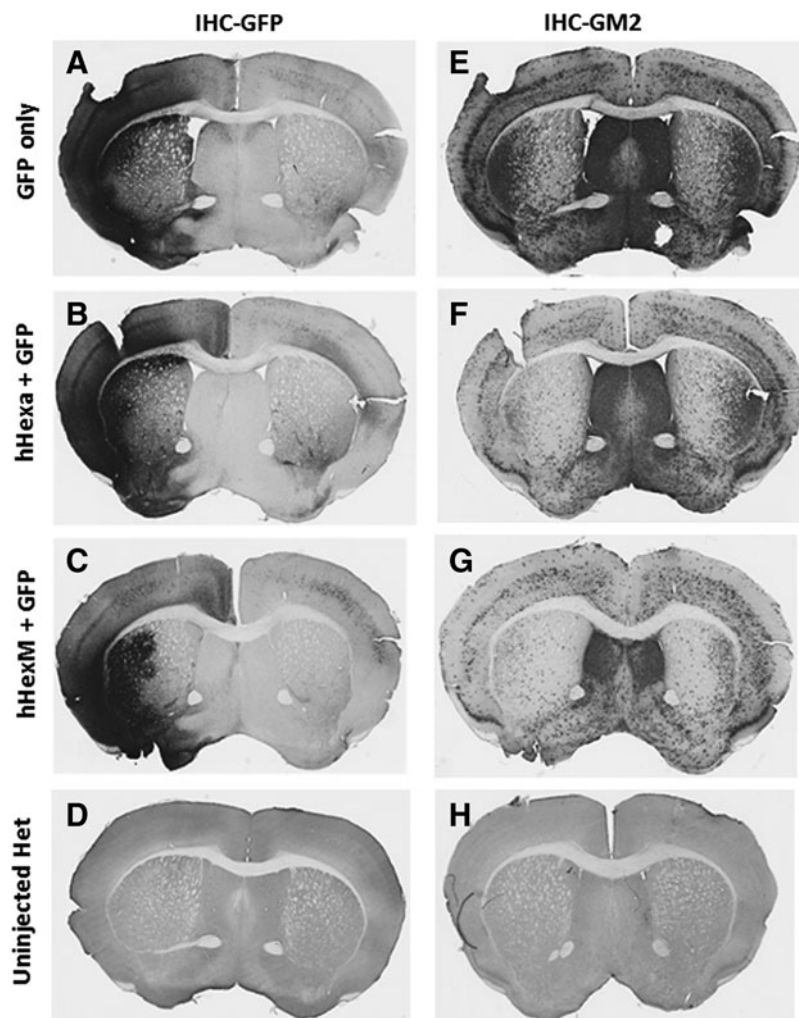
Figure 5. HexM is capable of reducing long-standing G_{M2} in aged Tay-Sachs mice. Fifteen-month-old TS knockout mice received a single unilateral intracranial injection of a two-vector mixture containing equal amounts of scAAV9/UsP-*GFP* and scAAV/UsP-*HEXA* or scAAV9/UsP-*HEXM*. They were killed 4 weeks postinjection and coronal sections of the brain were analyzed by IHC for GFP expression to indicate the spread of vector **(A–D)** and G_{M2} accumulation to assess the relative β-hexosaminidase activity **(E–H)**. Sections from the brain of an uninjected heterozygous mouse from the TS mouse colony were used as negative controls for both GFP expression and G_{M2} accumulation. The left side of mice was injected in **(A–C)** and **(E–G)**. The vector mixtures used are indicated on the left-hand side.

euthanized when 15 months old. The pattern of vector genome biodistribution when *HEXM* was the transgene was variable between individual mice but overall similar to the biodistribution pattern when GFP was the transgene (Fig. 6A; compare with Fig. 4A). Biochemical analysis of both rostral and caudal parts of the brain from treated mice showed a reduction in the accumulation of G_{M2} gangliosides compared with that of control uninjected TSD mice (Fig. 6B). The caudal (hind) brain had a more marked quantitative reduction in G_{M2} storage than the rostral brain (data not shown). This demonstrates the ability of the scAAV9.47/UsP-*HEXM* vector to mediate sustained reduction in CNS G_{M2} gangliosides, the hallmark of TSD pathology.

DISCUSSION

This paper addresses several challenges in creating an ideal gene replacement therapy for the related Tay-Sachs and Sandhoff diseases. Past studies have relied on single-stranded (ss)AAV, herpes simplex virus, or adenoviral vectors administered intracranially, to deliver a single Hex subunit with one vector or both subunits by a dual-vector approach.[7–10,12,14,37–41] One challenge is that the functional HexA enzyme consists of the α- and β-subunits, which from a gene transfer perspective complicates a simple gene replacement strategy because overexpression of one subunit will inevitably lead to the other endogenous subunit becoming rate-limiting. The *HEXM* gene, which
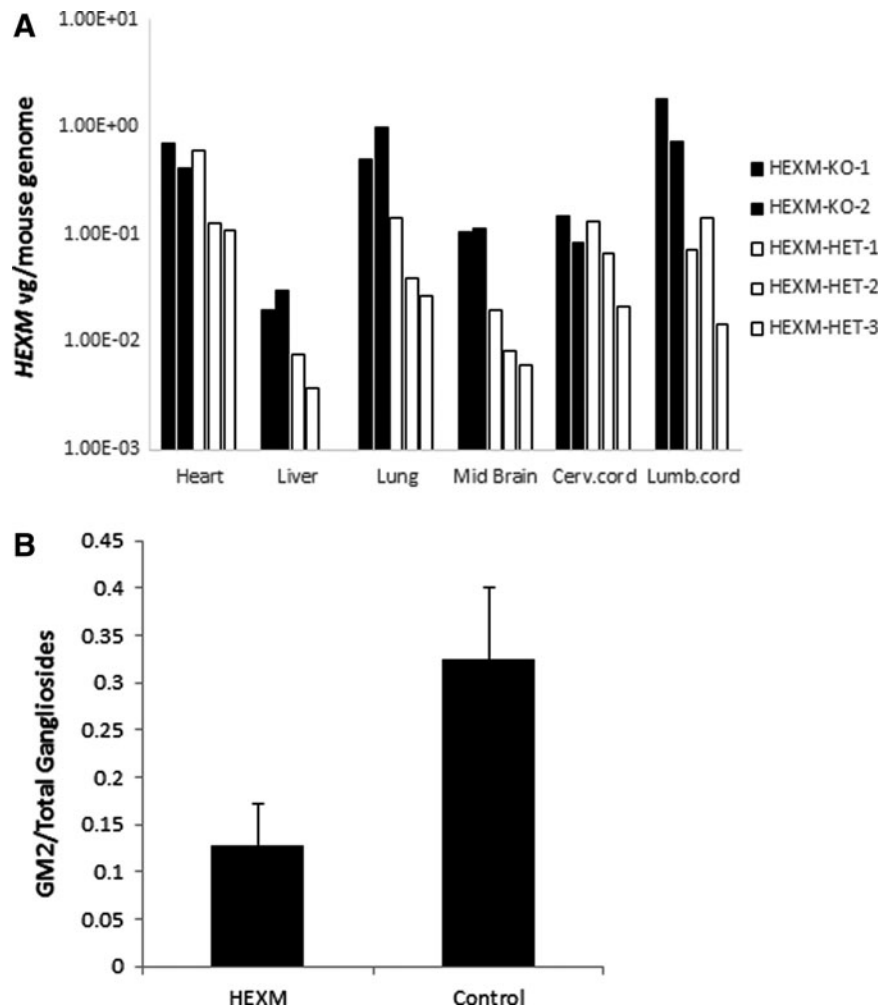
Figure 6. Intravenous administration of AAV9.47/UsP-*HEXM* in neonatal Tay-Sachs mice results in long-term reduction in G_{M2} ganglioside levels. Tay-Sachs mice, both knockout and heterozygous, were injected via the facial vein on P0–P2 with 5×10^{10} VG of scAAV9.47/UsP-*HEXM* and analyzed 15 months postinjection. **(A)** Vector biodistribution of scAAV9.47/UsP-*HEXM* in major organs from two KO and three heterozygous TSD mice. **(B)** The mean G_{M2}-to-total gangliosides ratio in the hindbrain region for neonatally injected *HEXM* ($n = 4$) and uninjected KO control ($n = 2$) mice. Error bars indicate the SEM.

encodes the modified Hex α-subunit variant, μ, overcomes this challenge because the Hex μ-subunit can form a stable homodimer, HexM, which functionally replaces the HexA heterodimer.[28] Overexpression of HexM has been shown to result in its enhanced secretion, and secreted HexM is taken up by other deficient cells through plasma membrane mannose 6-phosphate receptors. In addition, unlike HexA, both active sites in the HexM homodimer can potentially bind the $G_{M2}AP$–G_{M2} complex and hydrolyze G_{M2}. Thus, overexpression of HexM should exert a greater therapeutic benefit through cross-correction than would be possible through overexpression of either the α- or β-subunit alone, which would result predominantly in the secretion of either HexS or HexB, respectively. Furthermore, the *HEXM* gene can be packaged within a single scAAV vector, eliminating the need for a relatively inefficient dual-vector approach.

The *HEXA* and *HEXB* genes are each approximately 1.6 kb in length. Packaging them both within a single AAV vector is theoretically possible using traditional ssAAV vectors, but impossible within an scAAV vector. Strategies to achieve widespread CNS gene transfer in rodents, pigs, cats, dogs, and non-human primates have been described using AAV9, AAVrh10, and AAVrh8 vectors administered either intravenously or into the CSF, but these strategies rely on the more efficient scAAV.[16–19,21,34,42–49] The 1.6-kb size of the *HEXM* gene could potentially allow the *HEXM* gene to be packaged within an scAAV vector, making such a vector more amenable to these approaches for widespread CNS gene transfer. The selection of small promoters and poly(A) signals to package a 1.6-kb gene within the approximately 2.2-kb packaging constraints of scAAV is quite limited, so we employed a novel synthetic promoter–intron combination (UsP) based on the previously

described synthetic JeT promoter,[33] to provide a moderate level of expression when combined with the SV40 poly(A) signal. When driving GFP, the UsP construct displays similar ubiquitous expression throughout the CNS compared with the previously described CBh promoter,[22] although expression in astrocytes appears diminished somewhat. We conclude that the UsP promoter–intron, combined with the SV40 poly(A) signal, provides an ideal expression construct for *HEXM* within an scAAV vector.

A potential challenge related to intravenous administration of AAV vectors (AAV9, AAVrh10, or AAVrh8) targeting the CNS is that the high vector doses required also result in extraordinarily high loads of gene transfer to the liver. This creates the potential for deleterious liver-specific T cell responses,[50,51] possible toxicity related to transgene overexpression, and hepatocellular carcinoma when administered to neonates.[30,31] By using the AAV9.47 capsid, biodistribution to the liver was highly reduced relative to AAV9, while preserving the ability of AAV9 to cross the blood–brain barrier. An apparent reduction in astrocyte transduction with AAV9.47 was noted relative to AAV9, which may necessitate a slightly higher overall dose. However, in diseases that benefit from cross-correction, primary expression in neurons should be sufficient. Regarding the potential for hepatocellular carcinoma, our use of an enhancer-less expression construct would be expected to reduce the potential for oncogenesis. Whether as a result of the reduced liver biodistribution or the lack of an enhancer, our cohorts injected intravenously as neonates did not develop tumors up to their planned end point of 15 months old. Although this observation should be examined more carefully, it is encouraging. The time course of infantile TSD and SD in humans is rapid, and the earliest possible age of intervention would be ideal. Although it is unclear whether the risk of hepatocellular carcinoma with AAV vector observed in mice could translate to humans, our vector design potentially reduces that hypothetical risk.

The efficacy of gene therapy in mouse and cat models of G_{M2} gangliosidosis is susceptible to misinterpretation because of the sialidase metabolic bypass pathway, which could significantly reduce G_{M2} storage levels with any increase in hexosaminidase activity (i.e., HexA, HexB, HexS, or HexM). This bypass pathway does not exist in humans. The studies reported here were conducted in the TSD model, which is not ideal to evaluate treatment efficacy because of the mild phenotype of the mice. This paper provides information on the development of the reagents, along with evidence supporting the hypothesis that this has a likelihood of providing a therapeutic benefit. A companion article by Osmon and colleagues,[52] in this issue of *Human Gene Therapy* (see p. 497), describes the application of this approach and vector design with a mouse model of SD, which does display a severe disease phenotype, and is more appropriate for evaluating treatment efficacy.

Several technological advances were combined to generate a reagent to treat Tay-Sachs and Sandhoff diseases. This single scAAV vector design enables delivery approaches for widespread CNS gene transfer. Key to making use of scAAV are the novel hexosaminidase variant, *HEXM*, and the short synthetic promoter–intron UsP. Finally, by using an enhancerless expression construct and a liver-detargeted capsid, we suggest that the possible risk of hepatocellular carcinoma with this vector design would be greatly diminished. In conclusion, the collective body of work presented herein describes a novel vector design that greatly enhances the potential success of a gene transfer strategy to treat both Tay-Sachs and Sandhoff diseases. This vector design may also be useful to deliver other genes of similar size to treat CNS disorders.

ACKNOWLEDGMENTS

AUTHOR DISCLOSURE

REFERENCES

1. Sandhoff K, and Christomanou H. Biochemistry and genetics of gangliosidoses. Hum Genet 1979; 50:107–143.

2. Leinekugel P, Michel S, Conzelmann E, et al. Quantitative correlation between the residual activity of β-hexosaminidase A and arylsulfatase A and the severity of the resulting lysosomal storage disease. Hum Genet 1992;88:513–523.

3. Yamanaka S, Johnson MD, Grinberg A, et al. Targeted disruption of the *Hexa* gene results in mice with biochemical and pathologic features of Tay-Sachs disease. Proc Natl Acad Sci U S A 1994;91:9975–9979.

4. Sango K, Yamanaka S, Hoffmann A, et al. Mouse models of Tay-Sachs and Sandhoff diseases differ in neurologic phenotype and ganglioside metabolism. Nat Genet 1996;11:170–176.

5. Phaneuf D, Wakamatsu N, Huang JQ, et al. Dramatically different phenotypes in mouse models of human Tay-Sachs and Sandhoff diseases. Hum Mol Genet 1996;5:1–14.

6. Yuziuk JA, Bertoni C, Beccari T, et al. Specificity of mouse G_{M2} activator protein and β-*N*-acetylhexosaminidases A and B: similarities and differences with their human counterparts in the catabolism of G_{M2}. J Biol Chem 1998;273:66–72.

7. Guidotti JE, Mignon A, Hasse G, et al. Adenoviral gene therapy of the Tay-Sachs disease in hexosaminidase A-deficient knock-out mice. Hum Mol Genet 1999;8:831–838.

8. Cachon-Gonzalez MB, Wang SZ, Lynch A, et al. Effective gene therapy in an authentic model of Tay-Sachs-related diseases. Proc Natl Acad Sci U S A 2006;103:10373–10378.

9. Sargeant TJ, Wang S, Bradley J, et al. Adeno-associated virus-mediated expression of β-hexosaminidase prevents neuronal loss in the Sandhoff mouse brain. Hum Mol Genet 2011;20: 4371–4380.

10. Cachon-Gonzalez MB, Wang SZ, McNair R, et al. Gene transfer corrects acute G_{M2} gangliosidosis—potential therapeutic contribution of perivascular enzyme flow. Mol Ther 2012;20:1489–1500.

11. Bradbury AM, Gray-Edwards HL, Shirley JL, et al. Biomarkers for disease progression and AAV therapeutic efficacy in feline Sandhoff disease. Exp Neurol 2015;263:102–112.

12. Cachon-Gonzalez MB, Wang SZ, Ziegler R, et al. Reversibility of neuropathology in Tay-Sachs-related diseases. Hum Mol Genet 2014;23:730–748.

13. Weismann CM, Ferreira J, Keeler AM, et al. Systemic AAV9 gene transfer in adult G_{M1} gangliosidosis mice reduces lysosomal storage in CNS and extends lifespan. Hum Mol Genet 2015; 24:4353–4364.

14. Walia JS, Altaleb N, Bello A, et al. Long-term correction of Sandhoff disease following intravenous delivery of rAAV9 to mouse neonates. Mol Ther 2015;23:414–422.

15. Gadalla KK, Bailey ME, Spike RC, et al. Improved survival and reduced phenotypic severity following AAV9/*MECP2* gene transfer to neonatal and juvenile male *Mecp2* knockout mice. Mol Ther 2013;21:18–30.

16. Fu H, Dirosario J, Killedar S, et al. Correction of neurological disease of mucopolysaccharidosis IIIB in adult mice by rAAV9 trans-blood–brain barrier gene delivery. Mol Ther 2011;19:1025–1033.

17. Ruzo A, Marco S, Garcia M, et al. Correction of pathological accumulation of glycosaminoglycans in central nervous system and peripheral tissues of MPSIIIA mice through systemic AAV9 gene transfer. Hum Gene Ther 2012;23:1237–1246.

18. Gray SJ, Matagne V, Bachaboina L, et al. Pre-clinical differences of intravascular AAV9 delivery to neurons and glia: a comparative study of adult mice and nonhuman primates. Mol Ther 2011; 19:1058–1069.

19. Duque S, Joussemet B, Riviere C, et al. Intravenous administration of self-complementary AAV9 enables transgene delivery to adult motor neurons. Mol Ther 2009;17:1187–1196.

20. Mattar CN, Waddington SN, Biswas A, et al. Systemic delivery of scAAV9 in fetal macaques facilitates neuronal transduction of the central and peripheral nervous systems. Gene Ther 2013;20:69–83.

21. Foust KD, Nurre E, Montgomery CL, et al. Intravascular AAV9 preferentially targets neonatal neurons and adult astrocytes. Nat Biotechnol 2009;27:59–65.

22. Gray SJ, Foti SB, Schwartz JW, et al. Optimizing promoters for recombinant adeno-associated virus-mediated gene expression in the peripheral and central nervous system using self-complementary vectors. Hum Gene Ther 2011;22:1143–1153.

23. Powell SK, Rivera-Soto R, and Gray SJ. Viral expression cassette elements to enhance transgene target specificity and expression in gene therapy. Discov Med 2015;19:49–57.

24. Mark BL, Mahuran DJ, Cherney MM, et al. Crystal structure of human β-hexosaminidase B: understanding the molecular basis of Sandhoff and Tay-Sachs disease. J Mol Biol 2003;327:1093–1109.

25. Lemieux MJ, Mark BL, Cherney MM, et al. Crystallographic structure of human β-hexosaminidase A: interpretation of Tay-Sachs mutations and loss of G_{M2} ganglioside hydrolysis. J Mol Biol 2006; 359:913–929.

26. Matsuoka K, Tamura T, Tsuji D, et al. Therapeutic potential of intracerebroventricular replacement of modified human β-hexosaminidase B for G_{M2} gangliosidosis. Mol Ther 2011;19:1017–1024.

27. Sinici I, Yonekawa S, Tkachyova I, et al. *In cellulo* examination of a β–α hybrid construct of β-hexosaminidase A subunits, reported to interact with the G_{M2} activator protein and hydrolyze G_{M2} ganglioside. PLoS One 2013;8:e57908.

28. Tropak MB, Yonekawa S, Karumuthil-Melethil S, et al. Construction of a hybrid β-hexosaminidase subunit capable of forming stable homodimers that hydrolyze G_{M2} ganglioside *in vivo*. Mol Ther Methods Clin Dev 2016;3:15057.

29. Zincarelli C, Soltys S, Rengo G, et al. Analysis of AAV serotypes 1–9 mediated gene expression and tropism in mice after systemic injection. Mol Ther 2008;16:1073–1080.

30. Donsante A, Miller DG, Li Y, et al. AAV vector integration sites in mouse hepatocellular carcinoma. Science 2007;317:477.

31. Chandler RJ, LaFave MC, Varshney GK, et al. Vector design influences hepatic genotoxicity after adeno-associated virus gene therapy. J Clin Invest 2015;125:870–880.

32. Pulicherla N, Shen S, Yadav S, et al. Engineering liver-detargeted AAV9 vectors for cardiac and musculoskeletal gene transfer. Mol Ther 2011;19: 1070–1078.

33. Tornøe J, Kusk P, Johansen TE, et al. Generation of a synthetic mammalian promoter library by modification of sequences spacing transcription factor binding sites. Gene 2002;297:21–32.

34. Gray SJ, Nagabhushan Kalburgi S, McCown TJ, et al. Global CNS gene delivery and evasion of anti-AAV-neutralizing antibodies by intrathecal AAV administration in non-human primates. Gene Ther 2013;20:450–459.

35. Gray SJ, Choi VW, Asokan A, et al. Production of recombinant adeno-associated viral vectors and use in *in vitro* and *in vivo* administration. Curr Protoc Neurosci 2011;Chapter 4:Unit 4.17.

36. Seyrantepe V, Lema P, Caqueret A, et al. Mice doubly-deficient in lysosomal hexosaminidase A and neuraminidase 4 show epileptic crises and rapid neuronal loss. PLoS Genet 2010;6:e1001118.

37. Martino S, Marconi P, Tancini B, et al. A direct gene transfer strategy via brain internal capsule reverses the biochemical defect in Tay-Sachs disease. Hum Mol Genet 2005;14:2113–2123.

38. Gray-Edwards HL, Brunson BL, Holland M, et al. Mucopolysaccharidosis-like phenotype in feline Sandhoff disease and partial correction after AAV gene therapy. Mol Genet Metab 2015;116:80–87.

39. Rockwell HE, McCurdy VJ, Eaton SC, et al. AAV-mediated gene delivery in a feline model of Sandhoff disease corrects lysosomal storage in the central nervous system. ASN Neuro 2015;7(2).

40. McCurdy VJ, Rockwell HE, Arthur JR, et al. Widespread correction of central nervous system disease after intracranial gene therapy in a feline model of Sandhoff disease. Gene Ther 2015;22: 181–189.

41. Bourgoin C, Emiliani C, Kremer EJ, et al. Widespread distribution of β-hexosaminidase activity in the brain of a Sandhoff mouse model after coinjection of adenoviral vector and mannitol. Gene Ther 2003;10:1841–1849.

42. Duque SI, Arnold WD, Odermatt P, et al. A large animal model of spinal muscular atrophy and correction of phenotype. Ann Neurol 2015;77: 399–414.

43. Federici T, Taub JS, Baum GR, et al. Robust spinal motor neuron transduction following intrathecal delivery of AAV9 in pigs. Gene Ther 2011;19:852–859.

44. Meyer K, Ferrsiuolo L, Schmelzer L, et al. Improving single injection CSF delivery of AAV9-mediated gene therapy for SMA: a dose–response study in mice and nonhuman primates. Mol Ther 2015;23:477–487.

45. Passini MA, Bu J, Richards AM, et al. Translational fidelity of intrathecal delivery of self-complementary AAV9-survival motor neuron 1 for spinal muscular atrophy. Hum Gene Ther 2014;25:619–630.

46. Samaranch L, Salegio EA, San Sebastian W, et al. Strong cortical and spinal cord transduction after AAV7 and AAV9 delivery into the cerebrospinal fluid of nonhuman primates. Hum Gene Ther 2013;24:526–532.

47. Samaranch L, Salegio EA, San Sebastian W, et al. Adeno-associated virus serotype 9 transduction in the central nervous system of nonhuman primates. Hum Gene Ther 2012;23:382–389.

48. Haurigot V, Marco S, Ribera A, et al. Whole body correction of mucopolysaccharidosis IIIA by intracerebrospinal fluid gene therapy. J Clin Invest 2013;123:3254–3271.

49. Bucher T, Colle MA, Wakeling E, et al. scAAV9 intracisternal delivery results in efficient gene transfer to the central nervous system of a feline model of motor neuron disease. Hum Gene Ther 2013;24:670–682.

50. Nathwani AC, Tuddenham EG, Rangarajan S, et al. Adenovirus-associated virus vector-mediated gene transfer in hemophilia B. N Engl J Med 2011; 365:2357–2365.

51. Mingozzi F, and High KA. Immune responses to AAV in clinical trials. Curr Gene Ther 2007;7:316–324.

52. Osmon KJ, Woodley E, Thompson P, et al. Systemic gene transfer of a hexosaminidase variant using a scAAV9.47 vector corrects G_{M2} gangliosidosis in Sandhoff mice. Hum Gene Ther 2016; 27:497–508.